

Article

Syntheses, Structures, and Physical Properties of Neutral Gold Dithiolate Complex, [Au(etdt)₂] \cdot THF

Kazuha Sakaguchi, Biao Zhou *, Yuki Idobata, Hajime Kamebuchi and Akiko Kobayashi

Department of Chemistry, College of Humanities and Sciences, Nihon University, Sakurajosui 3-25-40, Setagaya-Ku, Tokyo 156-8550, Japan; sakakazu0309@gmail.com (K.S.); 6sided.currencystone@ezweb.ne.jp (Y.I.); hkame@chs.nihon-u.ac.jp (H.K.); akoba@chs.nihon-u.ac.jp (A.K.)

* Correspondence: zhou@chs.nihon-u.ac.jp; Tel.: +81-3-5317-9364

Received: 13 October 2020; Accepted: 3 November 2020; Published: 4 November 2020



Abstract: In order to develop new types of single-component molecular conductors with novel electronic structures and physical properties, the neutral gold dithiolate complex with an etdt (= ethylenedithiotetrathiafulvalenedithiolate) ligand, [Au(etdt)₂] was prepared. However, unlike the reported single-component molecular metals, the neutral gold complex [Au(etdt)₂] \cdot THF (**2**) contains a solvent molecule of tetrahydrofuran (THF). The crystals of **2** form a two-dimensional conducting layer structure, which are separated by the terminal ethylene groups and THF molecules. The fairly high room-temperature conductivity of 0.2 S/cm and semiconducting behavior with a low activation energy of 0.1 eV of **2**, is consistent with the result of the density functional theory band structure calculations. The observed non-magnetic behavior of **2** is caused from the dimeric structure of [Au(etdt)₂] molecules.

Keywords: single-component molecular conductors; extended-TTF dithiolate ligands; gold dithiolate complexes

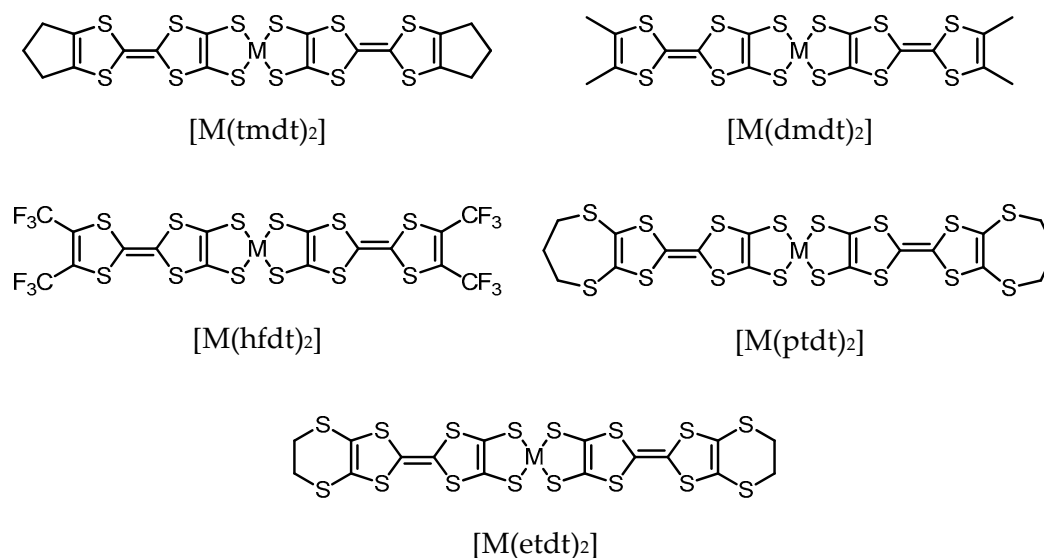
1. Introduction

Since the discovery of the first molecular metal, TTF-TCNQ (TTF = tetrathiafulvalene, TCNQ = tetracyanoquinodimethane) charge transfer complex in 1973 [1], many various types of molecular conductors have been reported, including famous examples such as (TMTSF)₂PF₆ (TMTSF = tetramethyltetraselenafulvalene)—the first molecular organic superconductor [2], and λ -(BETS)₂FeCl₄ (BETS = bis(ethylenedithio)tetraselenafulvalene)—a field induced superconductor [3,4]. These traditional charge transfer-based molecular conductors inherently consist of more than one kind of molecule, a donor as well as an acceptor. However, the first single-component molecular metal [Ni(tmdt)₂] (tmdt = trimethylenetetrathiafulvalenedithiolate) developed in 2001 has opened a new field of conducting materials [5,6]. [Ni(tmdt)₂] consists of only one kind of neutral molecule, and exhibits metallic behavior down to 0.6 K. The observation of de Haas-van Alphen oscillations, at very high magnetic fields and low temperatures, showed the existence of the three-dimensional Fermi surfaces [7], which was also proved by ab initio band structure calculations [8]. After that, a number of single-component molecular conductors have been reported, such as [Au(Me-thiazdt)₂] (Me-thiazdt = *N*-methyl-1,3-thiazoline-2-thione-4,5-dithiolate)—a single-component molecular metal without any TTF unit [9], and TED (= tetrathiafulvalene-extended dicarboxylate radical)—a single-component pure organic metal [10].

For single-component molecular conductor [M(L)₂] systems, an important characteristic is that its electronic structure can be widely tuned by exchanging the central transition metal atom (M) for another transition metal atom, even among isostructural systems. The series of isostructural systems, [M(tmdt)₂] (M = Ni, Cu, Pd, Pt, Au) is a typical case. [Ni(tmdt)₂] and [Pt(tmdt)₂] exhibit very high

conductivity and metallic behavior down to extremely low temperatures [11,12]. $[\text{Au}(\text{tmdt})_2]$ is a hybrid antiferromagnetic metal, and undertakes an antiferromagnetic transition at around 110 K as well as retaining its metallic state [13,14]. $[\text{Cu}(\text{tmdt})_2]$ is a hybrid Mott insulator, and shows a one-dimensional antiferromagnetic Heisenberg behavior with magnetic ordering at 13 K [15,16]. However, $[\text{Pd}(\text{tmdt})_2]$ with an even number of total electrons, is an antiferromagnetic semiconductor, and takes out a magnetic ordering onset exceeding 100 K due to strong electron correlation [17,18].

On the other hand, the difference of the ligands has an important effect or influence on the electronic structures and band structures of single-component molecular conductors. Actually, a variety of electronic structures have been realized by using similar extended-TTF dithiolate ligands with different terminal groups (as shown in Scheme 1). For example, unlike the isostructural $[\text{M}(\text{tmdt})_2]$ systems with a tight three-dimensional molecular packing, $[\text{M}(\text{ptdt})_2]$ ($\text{M} = \text{Ni}, \text{Au}$; ptdt = propylenedithiotetrathiafulvalenedithiolate) [19,20] and $[\text{M}(\text{hfdt})_2]$ ($\text{M} = \text{Ni}, \text{Au}, \text{Pd}$; hfdt = bis(trifluoromethyl)tetrathiafulvalenedithiolate) [21,22] crystallize in a layered two-dimensional (2D) molecular packing. Especially, $[\text{Ni}(\text{hfdt})_2]$ is a single-component molecular superconductor with transition temperatures at 5.5 K under high pressures around 8 GPa [23]. Recently, $[\text{Pt}(\text{dmdt})_2]$ has been found to host strongly correlated massless Dirac electrons with nodal lines at ambient pressure [24].



Scheme 1. Chemical structure of single-component molecular conductor $[\text{M}(\text{L})_2]$ systems mentioned in this paper.

It is well known that, for BEDT-TTF (= bis(ethylenedithio)tetrathiafulvalene) charge transfer complexes, the conformational flexibility of the terminal ethylene groups yields a variety of the crystal structures and the resultant electronic structures. For example, α -(BEDT-TTF) $_2\text{I}_3$ is a molecular Dirac electron system under high pressure [25], as well as β -, κ -, and θ -(BEDT-TTF) $_2\text{I}_3$ are ambient pressure molecular superconductors [26,27]. To develop new types of single-component molecular conductors with novel electronic structures and physical properties, we have tried to prepare a series of dithiolate complexes, with etdt (= ethylenedithiotetrathiafulvalenedithiolate) ligand, which contain the same terminal ethylene group to that of BEDT-TTF molecule. Although, some similar dithiolate complexes had been reported by G. Matsubayashi et al. [28,29], their oxidized neutral species have not been studied. We report here, syntheses, crystal structures, and physicals properties of new neutral gold dithiolate complexes, $[\text{Au}(\text{etdt})_2] \cdot \text{THF}$.

2. Materials and Methods

2.1. General Methods

All the syntheses were carried out under argon atmosphere using the Schlenk technique because the anionic state of metal complexes with extended-TTF dithiolate ligands are quite sensitive to oxygen. The etdt ligand [30] and the gold source, tetra-*n*-butylammonium tetrachloroaurate(III) (ⁿBu₄N·[AuCl₄]) [31], were prepared according to procedures reported in literature. Tetrahydrofuran (THF) was distilled over Na metal and benzophenone. Methanol (MeOH) was distilled over Mg metal activated with I₂. The supporting electrolytes tetra-*n*-butylammonium hexafluorophosphate (ⁿBu₄N·PF₆) used in the electrocrystallization was recrystallized three times with ethylacetate and dried in vacuo. All other reagents were used as purchased without any further purification.

2.2. Synthesis of ⁿBu₄N·[Au(etdt)₂] (1)

The etdt ligands (139 mg; 0.30 mmol) was hydrolyzed with a 25-wt% MeOH solution of tetramethylammonium hydroxide (Me₄N·OH) (440 mg; 1.2 mmol) in dry THF at room temperature. The solution was stirred for 30 min, and a reddish-orange intermediate precipitate was obtained as the reaction proceeded. After cooling to -78 °C in a dry ice/MeOH bath, a THF solution of ⁿBu₄N·[AuCl₄] (92 mg; 0.16 mmol) was added dropwise to the reaction mixture. Then, the reaction mixture was warmed to room temperature overnight. The resulting microcrystals were collected by filtration and crystallized from a THF solution of ⁿBu₄N·PF₆ at room temperature to afford dark-violet single crystals of **1**.

2.3. Electrochemical Synthesis of [Au(etdt)₂]·THF (2)

A mixture of **1** (~15 mg; 0.013 mmol) and ⁿBu₄N·PF₆ (100 mg; 0.26 mmol) as a supporting electrolyte was poured into H-shaped glass cells containing Pt electrodes and dissolved in dry THF (20.0 mL). When a constant current of 0.2 μA was applied at room temperature, air-stable black needle-like single crystals with sizes less than 80 μm of **2** grew on the Pt electrode within approximately 3 weeks.

2.4. Crystal Structure Determination of **1** and **2**

The single-crystal X-ray diffraction data for compounds **1** and **2** were collected on a Rigaku Micro7HFM-VariMax Saturn 724R CCD system equipped with graphite monochromated Mo K α radiation ($\lambda = 0.71073 \text{ \AA}$) and a confocal X-ray mirror. The crystal structures were solved using direct methods (SHELXT) [32] and refined by full-matrix least-squares (SHELXL) [33] under the Olex2 graphical interface [34]. Anisotropic temperature factors were applied for the non-hydrogen atoms. The calculated positions of the hydrogen atoms were not refined but included in the final calculations. The crystal data and experimental details of the crystal structure determination are listed in Table 1.

Table 1. X-ray crystallographic data of the gold complexes **1** and **2**.

	1	2
Empirical Formula	C ₃₂ H ₄₄ AuNS ₁₆	C ₂₀ H ₁₆ AuOS ₁₆
Formula Weight	1152.61	982.25
Crystal System	monoclinic	triclinic
Space Group	<i>P</i> 2 ₁ / <i>c</i> (#14)	<i>P</i> -1 (#2)
<i>a</i> /Å	20.7276 (5)	6.4340 (3)
<i>b</i> /Å	16.6751 (4)	8.6985 (4)
<i>c</i> /Å	12.7080 (3)	28.8338 (13)
α /°	90	84.332 (4)
β /°	90.421 (2)	87.668 (4)
γ /°	90	69.599 (4)
<i>V</i> /Å ³	4392.21 (18)	1505.07 (13)
<i>Z</i>	4	2
<i>D</i> _{calc} /g·cm ⁻³	1.743	2.167
Temp./K	173	298 (R.T.)
<i>F</i> (000)	2312	958
μ /mm ⁻¹	4.137	6.018
Reflections Collected	100,597	11,123
Independent Reflections	10,156	5934
Parameters	455	318
<i>R</i> ₁ (<i>I</i> > 2 σ) ¹	0.037	0.051
<i>wR</i> ₂ (all data) ²	0.074	0.138
GOF	1.013	1.104
CCDC	2,036,560	2,036,561

$$^1 R_1 = \sum ||F_o| - |F_c|| / \sum |F_o|. \quad ^2 wR_2 = [\sum \omega(|F_o| - |F_c|)^2 / \sum \omega F_o^2]^{1/2}.$$

2.5. Electrical Resistivity Measurements of **2**

Four-probe resistivity measurements were performed on compressed pellets of polycrystalline samples of **2** cooled by the liquid helium using a HECS 994C-1 multichannel four-terminal conductometer. Annealed gold wires (15 μ m in diameter) bonded to the sample by gold paint were used as leads.

2.6. Magnetic Measurements of **2**

Magnetic measurements of **2** were performed with a Quantum Design MPMS-7XL superconducting quantum interference device (SQUID) magnetometer in the temperature range of 2.0–300 K. The applied magnetic field was 5000 Oe. The samples were wrapped in clean aluminum foil whose magnetic susceptibility was separately measured and subtracted. The diamagnetic contribution was estimated from Pascal's constants.

2.7. Molecular Orbital, Band Structure, and Density of State Calculations of **2**

Molecular orbital (MO), band structure, and density of state (DOS) calculations were performed by density functional theory (DFT) and the general gradient approximation (GGA) method using the DMol³ module [35,36] as implemented in Materials Studio v5.5 (Accelrys, San Diego, CA, USA). Becke–Lee–Yang–Parr (BLYP) functional [37] and double numeric plus polarization (DNP) basis set were used in the calculations.

3. Results and Discussion

3.1. Crystal Structure of Monoanion Gold Complex **1**

Monoanion complex **1** crystallizes in monoclinic system with space group of *P*2₁/*c*. One tetra-*n*-butylammonium cation and one [Au(etdt)₂][−] anion are crystallographically independent in the unit cell. As shown in Figure 1a,b, the Au(III) atom in [Au(etdt)₂][−] anion shows a square-planar coordination

geometry, with Au-S distance of 2.316–2.326 Å, and an average S-Au-S angle of 91.30°, which is similar to those of the other reported gold dithiolate complexes [13,21]. The geometry of the two etdt ligands in $[\text{Au}(\text{etdt})_2]^-$ anion is not symmetrical: One of the ligands is almost planar, while the other ligand is bent at the positions of the outermost S atoms with a dihedral angle of 50.9°.

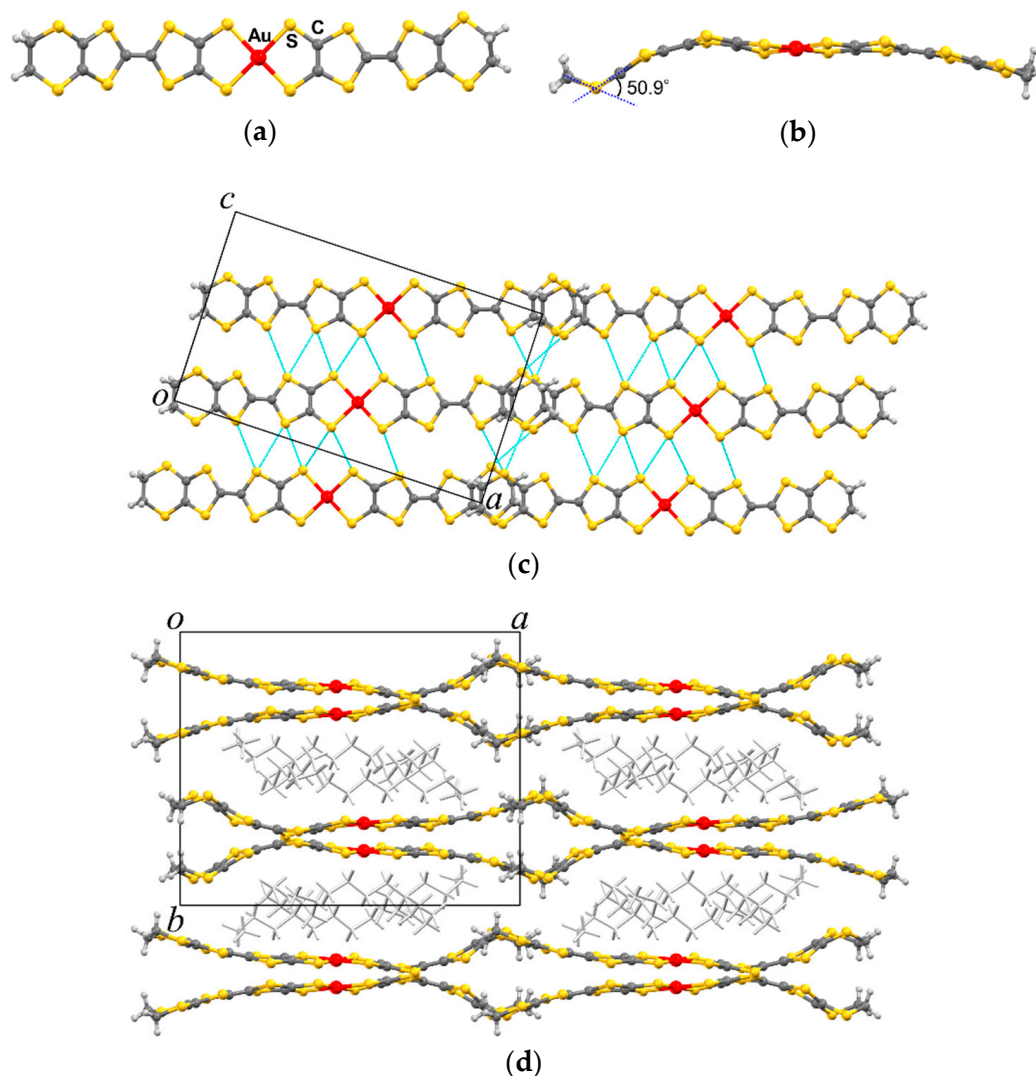


Figure 1. (a) Top view of the $[\text{Au}(\text{etdt})_2]^-$ anion. (b) Side view of the $[\text{Au}(\text{etdt})_2]^-$ anion. (c) Crystal structure of **1** viewed along the b -axis. The short S...S contacts (<3.7 Å) are shown as dotted line. The bulky tetra- n -butylammonium cations are omitted for clarity; (d) Crystal structure of **1** viewed along the c -axis.

As shown in Figure 1c, the $[\text{Au}(\text{etdt})_2]^-$ anions form side-by-side arrays along the c -axis with several short S...S contacts less than the sum of the van der Waals radii (<3.7 Å), with a shortest intermolecular S...S distance of 3.352 Å, indicating strong intermolecular interaction along the c -axis. On the other hand, the $[\text{Au}(\text{etdt})_2]^-$ anions are overlapped only on the terminal ethylene group along the long axis, to form a molecular layer parallel to the ac plane. As shown in Figure 1d, these molecular layers are separated by the bulky tetra- n -butylammonium cations along the b -axis. There is no short S...S contact between adjacent layers.

3.2. Crystal Structure of Neutral Gold Complex 2

Although the single crystal size is very small and thin, the crystal structure of neutral complex **2** has been successfully determined by single crystal X-ray structure analysis. The neutral complex **2** crystallizes into the triclinic system with space group of *P*-1. One neutral $[\text{Au}(\text{etdt})_2]$ molecule and one unexpected THF molecule are crystallographically independent in the unit cell. In traditional donor-acceptor molecular conductor systems, there are several examples reported which contain solvent molecules, such as β'' -(BEDT-TTF) $_4$ [(H₃O)Fe(C₂O₄)₃]·PhCN—the first paramagnetic molecular superconductor [38], (Me₄N)[Ni(ptdt)₂]·Me₂CO—a monoanion dithiolate nickel complex [19]. However, to the best of our knowledge, **2** is a rare case of solvent-containing neutral dithiolate complexes with extended-TTF ligands. Since **2** exhibits a distance of 3.240 Å between the oxygen atom of THF and ethylene groups of the etdt ligand (O··H-C), the THF molecules may be stabilized by the weak intramolecular hydrogen bonding. In general, solvent molecules do not contribute to the electronic structure, hence the neutral gold complex **2** is still single-component molecular conductor.

The molecular structure and the packing diagram viewed along the different axes of **2** are shown in Figure 2. The Au(III) atom in the neutral $[\text{Au}(\text{etdt})_2]$ molecule also show a square-planar coordination geometry, with Au-S distance of 2.318–2.336 Å, and an average S-Au-S angle of 91.10°, which is similar to that of **1**. The oxidized extended-TTF ligands in single-component molecular conductors usually became planar. However, as shown in Figure 2b, one of the etdt ligands in the neutral $[\text{Au}(\text{etdt})_2]$ molecule is still bent, which might be due to the space steric hindrance effect caused by the presence of THF molecules. On the other hand, the C=C distances in the TTF unit of the planar ligand are 1.340–1.360 Å, which is longer than that of **1**. Consequently, similar to that of reported single-component molecular conductors, the electrochemical oxidization was mainly carried out at the extended-TTF ligands.

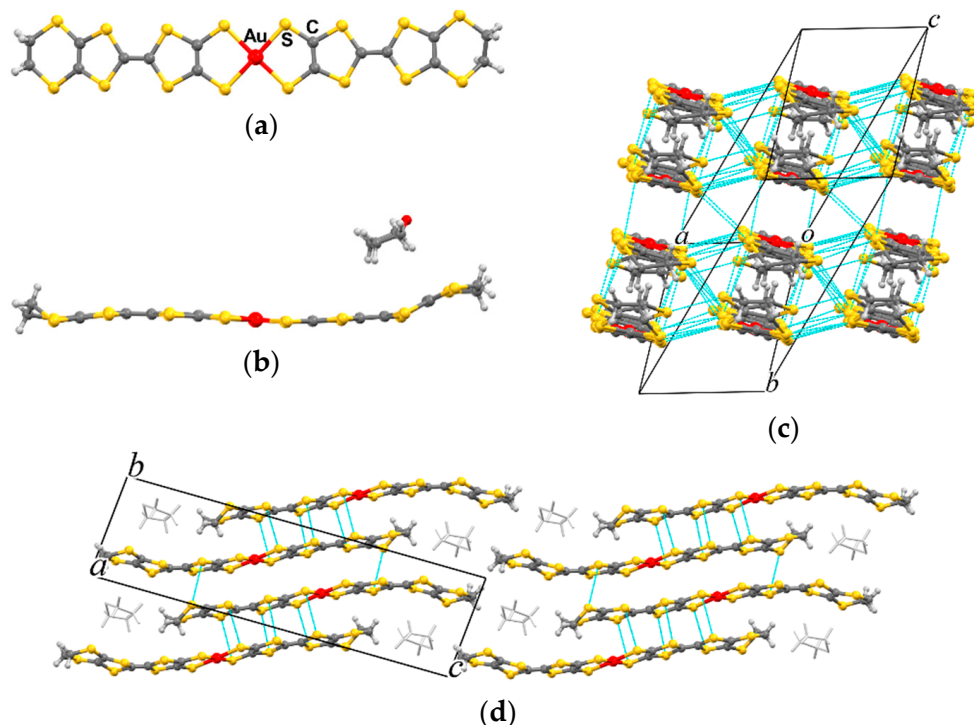


Figure 2. (a) Top view of the neutral $[\text{Au}(\text{etdt})_2]$ molecule without THF molecule. (b) Side view of the neutral $[\text{Au}(\text{etdt})_2]$ molecule with THF molecule. (c) Crystal structure of **2** viewed along the long axes of molecules. The short S··S contacts (<3.7 Å) are shown as dotted line. THF molecules are omitted for clarity. (d) Crystal structure of **2** viewed along the *a*-axis.

As shown in Figure 2c, the neutral $[\text{Au}(\text{etdt})_2]$ molecules are stacked face-to-face to form a dimeric column along the b -axis, with interplanar distances of 3.472 and 3.906 Å, respectively. The dimeric columns are arranged side-by-side along the a -axis to form a conduction layer parallel to the ab plane. There are many intermolecular S⋯S short contacts are observed in the molecular layer. Especially along the a -axis, a shortest intermolecular S⋯S distance of 3.394 Å suggests that **2** would be a satisfactory single-component molecular conductor with the relatively high conductivity. As shown in Figure 2d, the $[\text{Au}(\text{etdt})_2]$ conducting layers are strongly separated by the terminal ethylene groups and THF molecules along the c -axis, forming a 2D electronic structure. As mentioned before, such similar 2D electronic structure has also been observed in single-component molecular conductors with bulky ligands, $[\text{M}(\text{ptdt})_2]$ and $[\text{M}(\text{hfdt})_2]$.

3.3. Electrical Properties of Neutral Gold Complex **2**

Since the single crystal size of **2** was very small, resistivity measurements were performed by the standard four-probe method using compressed pellets of polycrystalline samples down to 40 K cooled by the liquid helium. The room-temperature conductivity (σ_{RT}) of **2** is about 0.2 S/cm, which is somewhat high for compressed pellet sample of 2D molecular conductor. As shown in Figure 3, the resistivity increases with decreasing temperature, and exhibits a semiconducting behavior with an activation energy (E_a) of about 0.1 eV in the temperature range of 200–300 K. Considering that the measurements were carried out on compressed pellets, **2** should be a fairly good conductor in the single crystalline state.

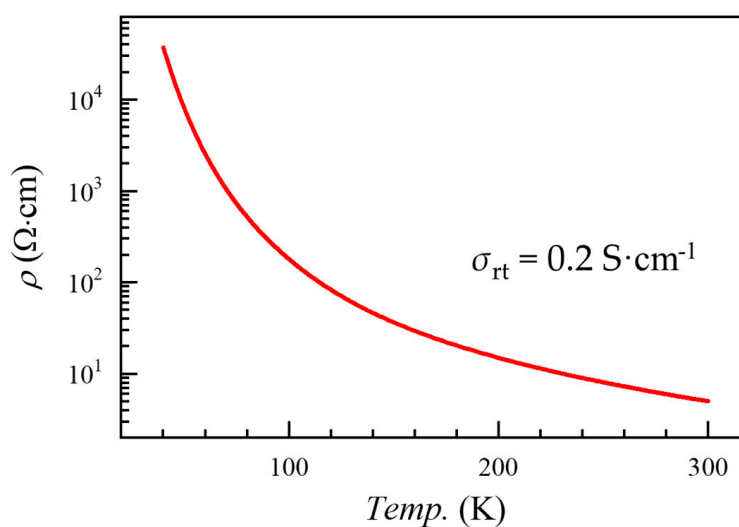


Figure 3. Temperature dependence of electrical resistivity of **2** measured by using compressed pellets.

3.4. Magnetic Susceptibility of Neutral Gold Complex **2**

The static magnetic susceptibilities of **2** were measured using a SQUID magnetometer at 5000 Oe in the temperature range of 2–300 K (Figure 4). After correction for the diamagnetic contribution of -4.0×10^{-4} emu/mol, the room-temperature susceptibility of **2** was almost zero (small than 2×10^{-5} emu/mol). The susceptibility values can be fitted well by the Curie–Weiss law over the entire temperature range, with a Curie constant of 2.2×10^{-3} K·emu/mol and a very small Weiss temperature of -0.15 K, which usually correspond to paramagnetic ($S_{1/2}$) impurities of 0.6%. Consequently, the magnetic susceptibility measurements suggest that **2** is essentially non-magnetic, which is consistent with the dimeric structure, and its semiconducting nature.

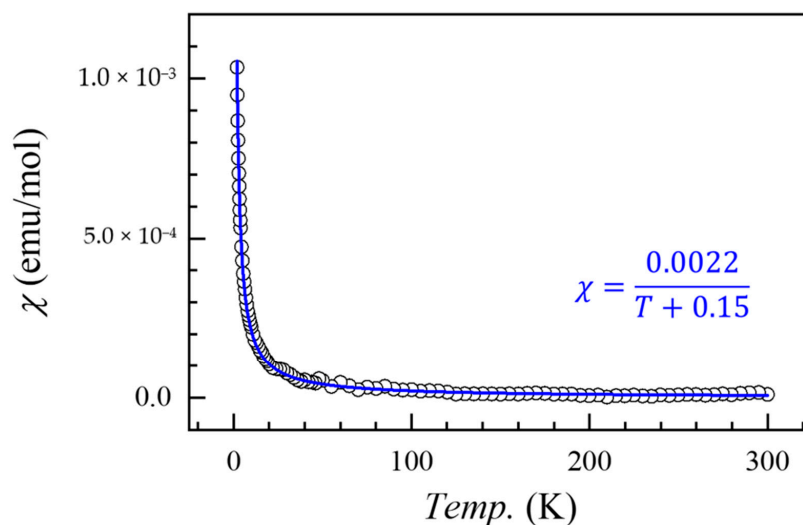


Figure 4. Temperature dependence of magnetic susceptibility of **2** at the field of 5000 Oe. The blue line is the Curie–Weiss fitting curve as described in the text.

3.5. Electronic Structures and Band Structure Calculations of Neutral Gold Complex **2**

The MO, band structure, and DOS calculations were performed by the DFT method. The spin polarized molecular orbitals and the energy levels of the neutral $[\text{Au}(\text{etdt})_2]$ molecule are shown in Figure 5a. The frontier orbitals near the Fermi level are very similar to those of reported gold dithiolate complexes with extended-TTF ligands, such as $[\text{Au}(\text{tmtdt})_2]$. The singly occupied molecular orbital (SOMO) of $[\text{Au}(\text{etdt})_2]$ is composed of an anti-symmetric combination of the left- and right-ligand π orbitals and a small contribution of the d orbital of the Au(III) atom. As a result, the spin density distribution of the $[\text{Au}(\text{etdt})_2]$ molecule shown in Figure 5b is mainly distributed on the ligand. As compared to the neutral $[\text{Au}(\text{tmtdt})_2]$, which becomes a magnetic metal exhibiting antiferromagnetic transition at 110 K, the neutral $[\text{Au}(\text{etdt})_2]$ becomes a non-magnetic semiconductor owing to the dimeric structure.

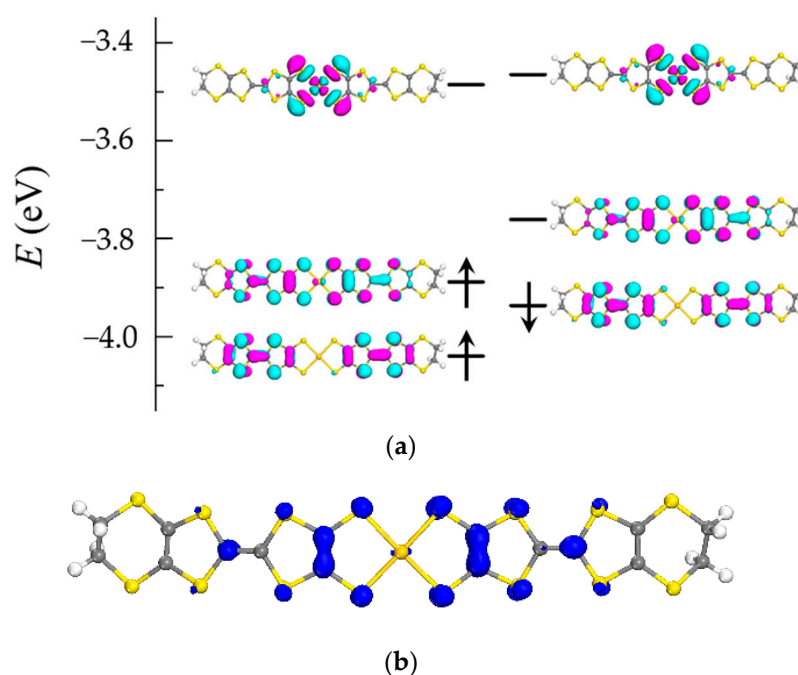


Figure 5. (a) Spin polarized molecular orbitals and the energy levels of the neutral $[\text{Au}(\text{etdt})_2]$ molecule. (b) Spin density distributions of the neutral $[\text{Au}(\text{etdt})_2]$ molecule.

The band energy dispersion curve and DOS of **2** are shown in Figure 6. The energy dispersion is very small along the c^* direction, but exhibits a considerable energy dispersion along the a^* and b^* directions, indicating the 2D nature of the system. The calculated DOS also give a band gap (ΔE) of about 0.20 eV, which is consistent with the semiconducting behavior and E_a ($\Delta E \approx 2E_a$) for the resistivity measurements.

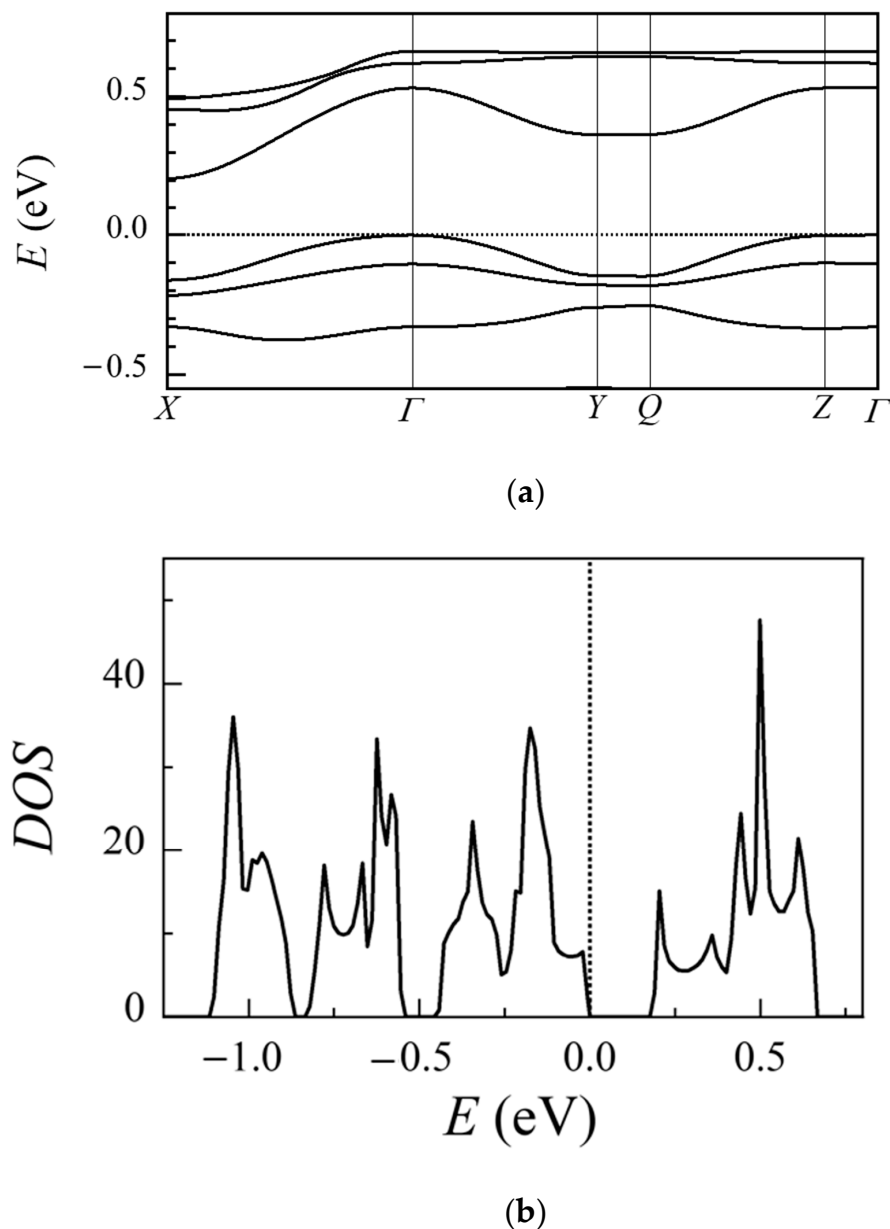


Figure 6. (a) The band energy dispersion curve of **2**. The symbols Γ , X, Y, Z, and Q represent the following positions in the reciprocal space: Γ (0,0,0), X ($1/2,0,0$), Y ($0,1/2,0$), Z ($0,0,1/2$), and Q ($0,1/2,1/2$). (b) The density of states (DOS) of **2**.

4. Conclusions

In conclusion, a new neutral gold dithiolate complex with an extended-TTF ligand, $[\text{Au}(\text{etdt})_2](\text{THF})$ (**2**), was prepared. Unlike the reported single-component molecular metals, **2** is a rare case of a solvent-containing single-component molecular conductor. The crystals of **2** are composed of 2D conducting layers of $[\text{Au}(\text{etdt})_2]$ molecules, which are strongly separated by the terminal ethylene groups and THF molecules. The resistivity measurements performed on the compressed pellets of

samples of **2** exhibit fairly high room-temperature conductivity of 0.2 S/cm and a low activation energy of 0.1 eV, which are consistent with the result of the DFT band structure calculations. The observed non-magnetic behavior of **2** is consistent with the dimeric structure of [Au(etdt)₂] molecules, and its semiconducting nature. Such results confirm that the crystal structures and electronic structures of the single-component molecular conductor [M(L)₂] system can be tuned by adopting various combinations of M and L.

Author Contributions: Conceptualization, B.Z. and A.K.; investigation, K.S., Y.I., B.Z. and A.K.; data curation, K.S., Y.I. and B.Z.; writing—original draft preparation, B.Z., H.K. and A.K.; writing—review and editing, B.Z., H.K. and A.K.; All authors have read and agreed to the published version of the manuscript.

Funding: This research was funded by “JSPS KAKENHI, grant number 17K05846”.

Acknowledgments: The authors would like to thank Nanotechnology Platform Program (Molecule and Material Synthesis) of MEXT, Japan.

Conflicts of Interest: The authors declare no conflict of interest.

References

1. Ferraris, J.; Cowan, D.O.; Walatka, V.; Perlstein, J.H. Electron transfer in a new highly conducting donor-acceptor complex. *J. Am. Chem. Soc.* **1973**, *95*, 948–949. [[CrossRef](#)]
2. Jérôme, D.; Mazaud, A.; Ribault, M.; Bechgaard, K.J. Superconductivity in a synthetic organic conductor(TMTSF)²PF₆. *Phys. Lett.* **1980**, *41*, 95–98.
3. Kobayashi, H.; Tomita, H.; Naito, T.; Kobayashi, A.; Sakai, F.; Watanabe, T.; Cassoux, P. New BETS Conductors with Magnetic Anions (BETS = bis(ethylenedithio)tetraselenafulvalene). *J. Am. Chem. Soc.* **1996**, *118*, 368–377. [[CrossRef](#)]
4. Uji, S.; Shinagawa, H.; Terashima, T.; Yakabe, T.; Terai, Y.; Tokumoto, M.; Kobayashi, A.; Tanaka, H.; Kobayashi, H. Magnetic-field-induced superconductivity in a two-dimensional organic conductor. *Nature* **2001**, *410*, 908–910. [[CrossRef](#)]
5. Tanaka, H.; Okano, Y.; Kobayashi, H.; Suzuki, W.; Kobayashi, A. Three-dimensional synthetic metallic crystal composed of single-component molecules. *Science* **2001**, *291*, 285–287. [[CrossRef](#)]
6. Kobayashi, A.; Fujiwara, E.; Kobayashi, H. Single-Component Molecular Metals with Extended-TTF Dithiolate Ligands. *Chem. Rev.* **2004**, *104*, 5243–5264. [[CrossRef](#)]
7. Tanaka, H.; Tokumoto, M.; Ishibashi, S.; Graf, D.; Choi, E.S.; Brooks, J.S.; Yasuzuka, S.; Okano, Y.; Kobayashi, H.; Kobayashi, A. Observation of Three-Dimensional Fermi Surfaces in a Single-Component Molecular Metal, [Ni(tmdt)₂]. *J. Am. Chem. Soc.* **2004**, *126*, 10518–10519. [[CrossRef](#)]
8. Rovira, C.; Novoa, J.J.; Mozos, J.-L.; Ordejón, P.; Canadell, E. First-principles study of the neutral molecular metalNi(tmdt)₂. *Phys. Rev. B* **2002**, *65*, 081104. [[CrossRef](#)]
9. Le Gal, Y.; Roisnel, T.; Auban-Senzier, P.; Bellec, N.; Íñiguez, J.; Canadell, E.; Lorcy, D. Stable Metallic State of a Neutral-Radical Single-Component Conductor at Ambient Pressure. *J. Am. Chem. Soc.* **2018**, *140*, 6998–7004. [[CrossRef](#)]
10. Kobayashi, Y.; Terauchi, T.; Sumi, S.; Matsushita, Y. Carrier generation and electronic properties of a single-component pure organic metal. *Nat. Mater.* **2017**, *16*, 109–114. [[CrossRef](#)]
11. Zhou, B.; Kobayashi, A.; Okano, Y.; Nakashima, T.; Aoyagi, S.; Nishibori, E.; Sakata, M.; Tokumoto, M.; Kobayashi, H. Single-Component Molecular Conductor [Pt(tmdt)₂] (tmdt = trimethylenetetrafulvalenedithiolate)—An Advanced Molecular Metal Exhibiting High Metallicity. *Adv. Mater.* **2009**, *21*, 3596–3600. [[CrossRef](#)]
12. Takagi, R.; Miyagawa, K.; Yoshimura, M.; Gangi, H.; Kanoda, K.; Zhou, B.; Idobata, Y.; Kobayashi, A. Magnetochiral nonreciprocity of volume spin wave propagation in chiral-lattice ferromagnets. *Phys. Rev. B* **2016**, *93*, 024403. [[CrossRef](#)]
13. Suzuki, W.; Fujiwara, E.; Kobayashi, A.; Fujishiro, Y.; Nishibori, E.; Takata, M.; Sakata, M.; Fujiwara, H.; Kobayashi, H. Highly Conducting Crystals Based on Single-Component Gold Complexes with Extended-TTF Dithiolate Ligands. *J. Am. Chem. Soc.* **2003**, *125*, 1486–1487. [[CrossRef](#)] [[PubMed](#)]

14. Hara, Y.; Miyagawa, K.; Kanoda, K.; Shimamura, M.; Zhou, B.; Kobayashi, A.; Kobayashi, H. NMR Evidence for Antiferromagnetic Transition in the Single-Component Molecular Conductor, [Au(tmdt)₂] at 110 K. *J. Phys. Soc. Jpn.* **2008**, *77*, 053706. [[CrossRef](#)]
15. Zhou, B.; Yajima, H.; Kobayashi, A.; Okano, Y.; Tanaka, H.; Kumashiro, T.; Nishibori, E.; Sawa, H.; Kobayashi, H. Single-Component Molecular Conductor [Cu(tmdt)₂] Containing an Antiferromagnetic Heisenberg Chain. *Inorg. Chem.* **2010**, *49*, 6740–6747. [[CrossRef](#)]
16. Takagi, R.; Hamai, T.; Gangi, H.; Miyagawa, K.; Zhou, B.; Kobayashi, A.; Kanoda, K. Single-component molecular material hosting antiferromagnetic and spin-gapped Mott subsystems. *Phys. Rev. B* **2017**, *95*, 094420. [[CrossRef](#)]
17. Ogura, S.; Idobata, Y.; Zhou, B.; Kobayashi, A.; Takagi, R.; Miyagawa, K.; Kanoda, K.; Kasai, H.; Nishibori, E.; Satoko, C.; et al. Antiferromagnetic Ordering in the Single-Component Molecular Conductor [Pd(tmdt)₂]. *Inorg. Chem.* **2016**, *55*, 7709–7716. [[CrossRef](#)]
18. Takagi, R.; Sari, D.P.; Mohd-Tajudin, S.S.; Ashi, R.; Watanabe, I.; Ishibashi, S.; Miyagawa, K.; Ogura, S.; Zhou, B.; Kobayashi, A.; et al. Antiferromagnetic Mott insulating state in the single-component molecular material Pd(tmdt)₂. *Phys. Rev. B* **2017**, *96*, 214432. [[CrossRef](#)]
19. Kobayashi, A.; Tanaka, H.; Kumasaki, M.; Torii, H.; Narymbetov, B.; Adachi, T. Origin of the High Electrical Conductivity of Neutral [Ni(ptdt)₂] (ptdt²⁻ = propylenedithiotetrathiafulvalenedithiolate): A Route to Neutral Molecular Metal. *J. Am. Chem. Soc.* **1999**, *121*, 10763–10771. [[CrossRef](#)]
20. Zhou, B.; Yajima, H.; Idobata, Y.; Kobayashi, A.; Kobayashi, T.; Nishibori, E.; Sawa, H.; Kobayashi, H. Single-component Layered Molecular Conductor, [Au(ptdt)₂]. *Chem. Lett.* **2012**, *41*, 154–156. [[CrossRef](#)]
21. Sasa, M.; Fujiwara, E.; Kobayashi, A.; Ishibashi, S.; Terakura, K.; Okano, Y.; Fujiwara, H.; Kobayashi, H. Crystal structures and physical properties of single-component molecular conductors consisting of nickel and gold complexes with bis(trifluoromethyl)tetrathiafulvalenedithiolate ligands. *J. Mater. Chem.* **2005**, *15*, 155–163. [[CrossRef](#)]
22. Zhou, B.; Ogura, S.; Liu, Q.Z.; Kasai, H.; Nishibori, E.; Kobayashi, A. A Single-component Molecular Conductor with Metal–Metal Bonding, [Pd(hfddt)₂] (hfddt = bis(trifluoromethyl)tetrathiafulvalenedithiolate). *Chem. Lett.* **2016**, *45*, 303–305. [[CrossRef](#)]
23. Cui, H.; Kobayashi, H.; Ishibashi, S.; Sasa, M.; Iwase, F.; Kato, R.; Kobayashi, A. A Single-Component Molecular Superconductor. *J. Am. Chem. Soc.* **2014**, *136*, 7619–7622. [[CrossRef](#)]
24. Zhou, B.; Ishibashi, S.; Ishii, T.; Sekine, T.; Takehara, R.; Miyagawa, K.; Kanoda, K.; Nishibori, E.; Kobayashi, A. Single-component molecular conductor [Pt(dmdt)₂]—A three-dimensional ambient-pressure molecular Dirac electron system. *Chem. Commun.* **2019**, *55*, 3327–3330. [[CrossRef](#)]
25. Kajita, K.; Nishio, Y.; Tajima, N.; Suzumura, Y.; Kobayashi, A. Molecular Dirac Fermion Systems—Theoretical and Experimental Approaches—. *J. Phys. Soc. Jpn.* **2014**, *83*, 072002. [[CrossRef](#)]
26. Kajita, K.; Nishio, Y.; Moriyama, S.; Sasaki, W.; Kato, R.; Kobayashi, H.; Kobayashi, A. New organic superconductors K- and θ-(BEDT-TTF)₂I₃: Transport property. *Solid State Commun.* **1987**, *64*, 1279–1284. [[CrossRef](#)]
27. Yagubskii, É.B.; Shchegolev, I.F.; Laukhin, V.N.; Kononovich, P.A.; Karatsovnik, M.V.; Zvarykina, A.V.; Buravov, L.I. Coexistence of different superconducting phases with transition temperatures between 1.5 and 7 K in the (BEDT-TTF)-I₃ system. *J. Exp. Theor. Phys.* **1984**, *39*, 12–16.
28. Nakano, M.; Kuroda, A.; Matsubayashi, G.-E. Extended bisdithiolene metal complexes: Preparation and electrical conductivities of [M(C₈H₄S₈)₂] anion complexes (M = Ni(II), Pt(II), Au(III)). *Inorg. Chim. Acta* **1997**, *254*, 189–193. [[CrossRef](#)]
29. Kubo, K.; Nakano, M.; Tamura, H.; Matsubayashi, G.-E.; Nakamoto, M. Preparation and oxidation of polarized Au(III) complexes having both the C-deprotonated-2-phenylpyridine (ppy) and a sulfur-rich dithiolate ligand and X-ray crystal structure of [Au(η²-C,N-ppy)(η²-S,S-C₈H₄S₈)]·0.5DMF. *J. Organomet. Chem.* **2003**, *669*, 141–148. [[CrossRef](#)]
30. Binet, L.; Fabre, J.M.; Montginoul, C.; Simonsen, K.B.; Becher, J. Preparation and chemistry of new unsymmetrically substituted tetrachalcogenofulvalenes bearing CN(CH₂)₂X and HO(CH₂)₂X groups (X = S or Se). *J. Chem. Soc. Perkin Trans. 1* **1996**, 783–788. [[CrossRef](#)]
31. Braunstein, P.; Clark, R.J.H. The preparation, properties, and vibrational spectra of complexes containing the AuCl²⁻, AuBr²⁻, and AuI²⁻ ions. *J. Chem. Soc. Dalton Trans.* **1973**, 1845–1848. [[CrossRef](#)]
32. Sheldrick, G. A short history of SHELX. *Acta Crystallogr. A* **2008**, *64*, 112–122. [[CrossRef](#)]

33. Sheldrick, G. SHELXT—Integrated space-group and crystal-structure determination. *Acta Crystallogr. C* **2015**, *71*, 3–8. [[CrossRef](#)]
34. Dolomanov, O.V.; Bourhis, L.J.; Gildea, R.J.; Howard, J.A.K.; Puschmann, H. OLEX2: A complete structure solution, refinement and analysis program. *J. Appl. Crystallogr.* **2009**, *42*, 339–341. [[CrossRef](#)]
35. Delley, B. An all-electron numerical method for solving the local density functional for polyatomic molecules. *J. Chem. Phys.* **1990**, *92*, 508–517. [[CrossRef](#)]
36. Delley, B. From molecules to solids with the DMol3 approach. *J. Chem. Phys.* **2000**, *113*, 7756–7764. [[CrossRef](#)]
37. Perdew, J.P.; Burke, K.; Ernzerhof, M. Generalized Gradient Approximation Made Simple. *Phys. Rev. Lett.* **1996**, *77*, 3865–3868. [[CrossRef](#)]
38. Kurmoo, M.; Graham, A.W.; Day, P.; Coles, S.J.; Hursthouse, M.B.; Caulfield, J.L.; Singleton, J.; Pratt, F.L.; Hayes, W.; Ducasse, L.; et al. Superconducting and Semiconducting Magnetic Charge Transfer Salts: (BEDT-TTF)₄AFe(C₂O₄)₃·n·C₆H₅CN (A = H₂O, K, NH₄). *J. Am. Chem. Soc.* **1995**, *117*, 12209–12217. [[CrossRef](#)]

Publisher’s Note: MDPI stays neutral with regard to jurisdictional claims in published maps and institutional affiliations.



© 2020 by the authors. Licensee MDPI, Basel, Switzerland. This article is an open access article distributed under the terms and conditions of the Creative Commons Attribution (CC BY) license (<http://creativecommons.org/licenses/by/4.0/>).